JOC The Journal of Organic Chemistry

Albright COLLEGE

Subscriber access provided by ALBRIGHT COLLEGE

Article

Electrosynthesis of N-methylisatin

Jaime Fernando Martínez Suárez, Jose A. Caram, Gustavo A. Echeverría, Oscar E. Piro, Ana María Gennaro, and Maria Virginia Mirifico

J. Org. Chem., **Just Accepted Manuscript** • DOI: 10.1021/acs.joc.9b00690 • Publication Date (Web): 14 May 2019

Electrosynthesis of N-methylisatin

Jaime F. Martínez Suárez,[a] José A. Caram,[a] Gustavo. A. Echeverría,[b] Oscar E. Piro,[b] Ana. M. Gennaro[c] and María. V. Mirífico[*,a,d]

[a] Instituto de Investigaciones Fisicoquímicas Teóricas y Aplicadas (INIFTA), CONICET-CCT La Plata, Facultad de Ciencias Exactas, Departamento de Química, Universidad Nacional de La Plata, Casilla de Correo 16, Sucursal 4, 1900 La Plata, Argentina.

[b] Departamento de Física, Facultad de Ciencias Exactas, Universidad Nacional de La Plata e Instituto IFLP (CONICET, CCT-La Plata), C. C. 67, 1900 La Plata, Argentina.

[c] Instituto de Física del Litoral, UNL-CONICET. Güemes 3450, 3000 Santa Fe, Argentina, and Departamento de Física, Facultad de Bioquímica y Ciencias Biológicas, Universidad Nacional del Litoral, Santa Fe, Argentina.

[d] Facultad de Ingeniería, Departamento de Ingeniería Química, Universidad Nacional de La Plata, Calle 47 y 1, 1900 La Plata, Argentina.

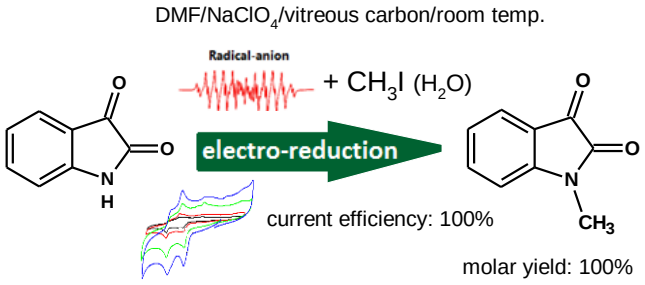

ABSTRACT: Isatin in a solution of dry DMF/$NaClO_4$ is electro-reduced in the presence of CH_3I. N-methylisatin (NMI) is obtained in quantitative molar yield and high current efficiency by controlled potential electrolysis (CPE). NMI and N-methylisatoic anhydride are the reaction products when CPE is performed in the absence of CH_3I, but adding it once the CPE was completed. The water effect on the identity and yield of the reaction product(s) is investigated. Reaction pathways are proposed.

INTRODUCTION

Isatin (indoline-2,3-dione; ISH in Figure 1) and its derivatives are important compounds found in natural products and in many bioactive molecules with anticancer,[1,2] anticonvulsants[3] and other antiviral,[4,5] antibacterial and antifungal properties.[6] ISH is used in the synthesis of oligo/polymeric structures with applications in the field of organic electronic devices.[7–12] Furthermore, ISH seems to be a promising molecule in the field of liquid crystals and crystal engineering because of its molecular structure with convenient characteristics (moderately large dipole moment and notable hydrogen bond donor/acceptor abilities) for the construction of supramolecular assemblies.[13] The importance of the indole derivatives in different fields has encouraged researchers to develop synthetic methods for their preparations.[14–17] N-methylisatin (1-methylindoline-2,3-dione; NMI in Figure 1) derivative presents cytotoxic, antinociceptive and cytoprotective activity.[18–20] Some carbazone and hydrazone derivatives have virus inhibition capacity, antimicrobial and/or antioxidant activity *in vitro* tests.[21–23] NMI has been used as a precursor in the synthesis of quinolone, quinoxaline, spiro compounds, Schiff and Mannich bases,[24-34] polymers and indigoids dyes.[24–26] Reduction of NMI with sodium amalgam gives a compound with characteristics of organic electron donor.[27] Furthermore, NMI nanoparticles have been used as a novel probe for selective detection of Cd^{2+} ion in aqueous medium.[28]

It is well known that ISH, (cyclic alpha-ketoamide) and common alkylating agents (alkyl halides or sulphates) do not react by simple contact between them. To alkylate the ISH molecule by the generally used procedures it is necessary to generate the isatin anion (IS^-) which is then treated with the alkylating agent. Direct synthesis of *N*-alkylisatins from *N*-alkylanilines and the *N*-alkylation of ISH employing a base are the commonly used procedures.[29–31] Direct synthesis is a multi-step procedure that generally gives *N*-alkylisatins in moderate to low yields.[32] For the *N*-alkylation of ISH different bases (NaOH, K_2CO_3, CaH_2, NaH, etc.) and solvents are used for the generation of IS^-. The different methods give good yields of

N-alkylisatins in some cases, but present certain disadvantages as the alkaline hydrolysis of the amide chemical function in some isatins or *N*-alkylisatins,[33,34] the need of anhydrous solvents due to the use of dangerous reagents such as metal hydrides, and/or long reaction times and side products formation that difficult the isolation of the desired product.[31] For example, the above mentioned amide hydrolysis is reported by Torisawa *et al.*[35] for 5-nitroisatin.

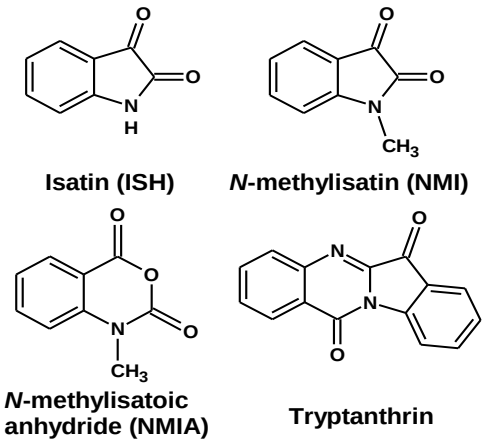

Figure 1. Structural formulas of isatin, *N*-methylisatin, *N*-methylisatoic anhydride, and tryptanthrin.

Electrochemical technology can be used to replace toxic or dangerous oxidizing/reducing reagents and also for the *in-situ* production of unstable and hazardous reagents. Electrosynthesis is considered a clean and efficient synthetic methodology. When using the electron as a reagent the number of steps is reduced as compared to conventional thermal processes, cleaner reaction mixtures are obtained, the isolation of the product is simpler, and the pollution caused by the use of chemicals is decreased.[36-40] Stimulated by the recent achievements in electroorganic synthesis,[38] in this work we study the electrochemical reduction of ISH in DMF solution at preparative scale (*see* SI) as a new and clean methodology for NMI synthesis. The electrolysis (controlled potential electrolysis, CPE) was performed under different experimental conditions (Table 1). The water effect on the identity and molar yield of the reaction product(s) is investigated. Current efficiency and cyclic voltammetric results are presented, and mechanistic proposals based on qualitative/quantitative products analysis/current efficiency are discussed. The peculiarities of the NMI molecule structure and crystal packing are studied by single crystal X-ray diffraction.

RESULTS AND DISCUSSION

Table1. Experimental conditions and results of controlled potential electrolysis (CPE)

Experimental conditions (EC)[a]		time[d] (min)	Products	Molar yield (%)	Current efficiency[e] (%)
EC**1**[b]	without H_2O	115	NMI	100	100
	with H_2O	515	NMI	100	49.3
EC**2**[c]	without H_2O	165	NMI; NMIA	49.8 50.2	61.5
	with H_2O	330	NMI; NMIA	46.5 53.5	78.0

[a]CPEs of ISH (9.66 mM) in $NaClO_4$ (0.1M)/DMF solution/C-vitreous electrode. Eappl= -1.35 V *vs.* Ag^+ (0.1 M, ACN)/Ag°. [b]EC**1**: CPE with CH_3I (15,1 mM). Experiments with [H_2O]: 50.3 mM. [c]EC**2**: CPE without CH_3I and further addition of CH_3I (15.1 mM). Experiments with [H_2O]: 50.3 mM. [d]Electrolysis time. [e]Current efficiency (%) was calculated based on the number of electrolyzed ISH mmoles.

Cyclic voltammograms (CVs) of ISH in DMF/$NaClO_4$ solution/C-vitreous electrode, without CH_3I and H_2O, were measured previously to the preparative experiments to choose the best conditions to obtain NMI and for information about the possible reaction mechanism. Up to four cathodic peaks (cp1-4) can be observed in the CVs measured without CH_3I in the electrolyte solution according to the ISH initial concentration (1.0 - 51.6 mM) and the potential scan rate (*v*: 0.020-0.500 V/s). At *v*: 0.200 V/s and 6.45-12.9 mM ISH, the peak potentials are Ecp1: -1.30 V; Ecp2: -1.47 V; Ecp3: -1.70 V and Ecp4: -1.87 V. The CV measured without CH_3I in the electrolyte solution (Figure 1S) shows a mono-electron quasi-reversible redox couple (cp1/ap1) when the potential scan includes only the first couple. $\Delta Ep = Eap1 - Ecp1 = 70/n$ mV (the value for an ideal reversible process is 59/n mV).[41] This result suggests that the radical-anion $ISH^{\bullet -}$ is formed in cp1[42,43] at Ecp1 (Scheme 1). However, potential scan rate dependence is shown by the CVs when the potential is scanned to more cathodic zones. For the slowest *v* the CV shows the cp2 at E_{cp2} (Figure 2S). As the potential is scanned at a higher *v*, the cp2 seems to disappear (Figure 2S) until it is no longer observed at the highest investigated rate. The possible superposition of the cp2 with the cp1 is neglected because the current intensity of the cp1 (Icp1) is linearly proportional to $v^{1/2}$ (Figure 3S). This behavior suggests that a chemical reaction (C, Scheme 1) is taking place. We propose that this homogeneous reaction produces the radical $ISH_2^{\bullet}$ and the anion IS^- whose concentrations are dependent on ISH initial concentration (Figure 4S), as will be discussed below. The mono-electronic electro-reduction of the radical $ISH_2^{\bullet}$ to the anion ISH_2^- occurs at E_{pc2} (Figures 2S and 4S). As it was mentioned above, there is an effect of ISH initial concentration on the electrochemical behavior of ISH. Only two cathodic processes, cp1 and cp4 (Figure 4S), are observed for the lowest concentration of ISH. As the concentration of ISH in the electrolyte medium increases, cp3 begins to be detected at Ecp3 (Figure 4S) and remains at the highest concentration, while cp4 disappears, being no longer observed at the highest investigated concentration. The cp4 (Figures 2S and 4S) corre-

sponds to the mono-electronic reduction of $ISH^{\bullet -}$ to the dianion ISH^{2-} (E4, Scheme 1). The Icp4 is linearly proportional to $v^{1/2}$, and it is diffusion controlled (Figure 3S). The Ecp3 is similar to that measured for ISH in DMF/$NaClO_4$ solution in the presence of KOH, in a molar ratio ISH/KOH *ca.* 1 (Figure 5S). Hence, cp3 is assigned to the reduction of the IS^- anion (Figure 4S), and this is confirmed by the absence of cp4 for the lowest ISH concentration. The cp3 is only observable for the highest initial ISH concentrations (12.9 – 51.6 mM). The described behavior is rationalized as the result of the chemical reaction C (Scheme 1), slow on the CV time scale, following the first charge transfer.

Scheme 1. Mechanism for electro-reduction of ISH in DMF/$NaClO_4$

E1;	$ISH + 1e^- \leftrightarrows ISH^{\bullet -}$	Ecp1: -1.30 V
C ;	$ISH^{\bullet -} + ISH \rightarrow ISH_2^{\bullet} + IS^-$	*slow*
E2;	$ISH_2^{\bullet} + 1e^- \rightarrow ISH_2^-$	Ecp2: -1.47 V
E3;	$IS^- + 1e^- \rightarrow IS^{\bullet 2-}$	Ecp3: -1.70 V
E4;	$ISH^{\bullet -} + 1e^- \rightarrow ISH^{2-}$	Ecp4: -1.87 V

The ESR spectrum (Figure 2) of a solution of ISH/DMF/$NaClO_4$ electrolyzed for a short period of time (15 min) shows the existence of a paramagnetic species, which is identified as $ISH^{\bullet -}$ by spectral simulation (Figure 2). Hyperfine interaction of the free electron with the nitrogen nucleus and five non-equivalent protons is evidenced in the ESR spectrum (fit: 0.108 mT (1N); 0.377 mT (1H); 0.319 mT (1H); 0.025mT (1H); 0.098 mT (1H) and 0.109 mT (1H); g factor = 2.0044. The radical-anion $ISH^{\bullet -}$ disappears during the course of the CPE as shown by the disappearance of the oxidation peak corresponding to the transformation of $ISH^{\bullet -}$ in ISH in the registered CV for 175 min of electrolysis (Figure 6S). This observation suggests that the chemical step C (Scheme 1) also occurs during the CPE performed at the potential of the first reduction charge transfer. Accordingly, $ISH_2^{\bullet}$ is more difficult to be reduced than ISH, because if the neutral radical was reduced at Ecp1 as might be supposed[44,45] and the homogeneous reaction was occurring, the non-paramagnetic species ISH_2^- would exist in the solution electrolyzed for large periods of time.

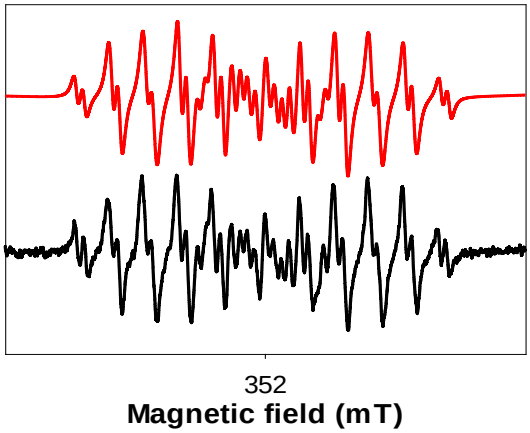

Figure 2. ESR spectrum recorded after the electrolysis (E_{appl}= -1.35V) of a 4.3 mM ISH/DMF/0.1 M $NaClO_4$ solution, for a short time (15 min). Experimental (——) and fitted (——) spectra.

The important differences on the CV behavior of ISH in DMF/$NaClO_4$ solution on carbon vitreous electrode between the results of our work and those published in the literature are the detection and stability of the species formed, and not the type of species generated during the electrode processes. Gupta and Sindal[43], working in solution of DMF/LiCl as supporting electrolyte system on a hanging mercury drop electrode, observed two separated one electron transfer waves. They propose that the first electron transfer leads to the formation of the radical $ISH^{\bullet -}$ and that the electro-reduction of $ISH_2^{\bullet}$ formed by the homogeneous reaction C (Scheme 1) also occurs at the potential of the first wave, whereas the second one leads to dioxindole by conducting controlled potential coulometry. However, our work shows that $ISH_2^{\bullet}$ is electro-reduced at a more cathodic potential with respect to the initial organic substrate (Scheme 1). We show that the reduction of $ISH_2^{\bullet}$ to ISH_2^- does not occur at Ecp1 because if this was the situation, the ESR would not show a signal because ISH_2^- instead of the radical anion would be the species present in the medium. However, the different behavior is rationalized by a competition between the electro-generated base (ISH_2^-) and the solvent (Solv) by the cation of the supporting electrolyte (Na^+ or Li^+): $Na^+/Li^+[Solv] + ISH_2^- \leftrightarrows Solv + Na^+/Li^+[ISH_2^-]$. This is a homogeneous equilibrium reaction subsequent to the charge transfer $ISH_2^{\bullet}/ISH_2^-$, and the greater the value of the equilibrium constant, the greater the Ecp2 displacement to less cathodic potentials should be observed in the measured CV, as it is suggested by Gupta and Sindal.[43] Li^+ tends to join the electrochemical processes of reduction,[46,47] which sometimes makes it difficult to separate consecutive processes of electronic transfer. Except for this aspect, Li^+ does not present other significant difference with respect to Na^+. The second aspect is the detection of the IS^- reduction, which was observed for ISH concentrations higher than *ca.*13 mM (Figure 4S), showing that the homogeneous reaction (C, Scheme 1) is dependent on the initial concentration of ISH. The comparison of our results with those from Gupta and Sindal,[43] leads to the choice of the sodium salt and not a lithium one to be selected as supporting electrolyte to obtain the desired NMI product.

The presence of CH_3I in the electrolyte solution causes some changes in the CV of ISH compared to the voltammogram measured in the absence of the methylating agent. On the one hand, an increase in the cathodic current intensity for potentials lower than *ca.* -2 V because of the electro-activity of CH_3I at these cathodic potentials is observed (CV of CH_3I not shown). Also, the CV scanned (*v*: 0.200 V/s) including only the cp1 shows a decrease in the current intensity of ap1 in the reverse anodic scan for ISH initial concentration *ca.* 10 mM (Figure 7S). This behavior suggests that both $ISH^{\bullet -}$ and/or IS^- (Scheme 1) could react with CH_3I in homogeneous phase. However, the circulated charge in a CPE experiment corresponds to a number of mole of e^-/mole of ISH *ca.* 1, and 1 mole of NMI is formed/1 mole ISH electrolyzed (Table 1). Then, at least in CPE experiments performed with the methylating agent in the electrolyte solution, the nucleophilic species seems to be $ISH^{\bullet -}$ and not IS^-. $ISH^{\bullet -}$ is sufficiently stable in DMF to be detected and measured by CV (Figures 4S and 6S) and ESR even if the sample was transferred into the ESR cavity after electrolysis outside (Figure 2). However, Batanero and Barba[48] rationalized the electro-reduction ISH in DCM solution at a Pt or Hg through a first mono-electronic charge transfer with hydrogen evolution to the corresponding IS^-

anion. According to our knowledge, these authors do not inform experiments performed to detect or measure the hydrogen evolution. We consider that the different behavior of the $ISH^{\bullet -}$ is the result of the solvent effect on the radical anion stability. It is known that solvation contributes to the stability of radical anions.[49] Radical anions are especially sensitive to medium effects. A more exhaustive discussion of the solvent effect on the stability of radical anions is presented, for example in ref. 50. On the other hand, Farinia *et al.*[51] published that the radical anion ($ISH^{\bullet -}$) which is formed in the first charge transfer step can react with ISH itself in a protonation reaction. The neutral radical formed can immediately add a second electron. That is, they propose the same chemical reaction "C" that we propose in our manuscript, but not the fast hydrogen evolution as Batanero and Barba suggest.[48]

The CVs measured for the residual solids isolated (*see* experimental section) from the electrolyzed solutions (Figure 3) show three quasi-reversible cathodic peaks at -1.43, -1.98 and -2.35 V if the CPE was performed without CH_3I added to the electrolytic medium, and only two reversible cathodic peaks at-1.42 and -2.00 V, if the CPE was performed in the presence of an excess of the methylating agent. The two less cathodic peaks correspond to NMI measured in the same electrolyte medium (Figure 8S).

The identification and quantification of the reaction products were simultaneously performed by GC-MS peaks and the areas of the ion peaks, respectively. One or two peaks at m/z 161.0 and 177.0 corresponding to NMI and N-methylisatoic anhydride (NMIA) with retention time 9.94 and 11.71 min, respectively (*e.g.* Figure 9S and Table 1S for the EC2 in Table 1) are shown in the chromatograms of the residual solids after the workup of the electrolyzed solutions. The quantification of the products was carried out by means of the external standard method, using ISH as standard.

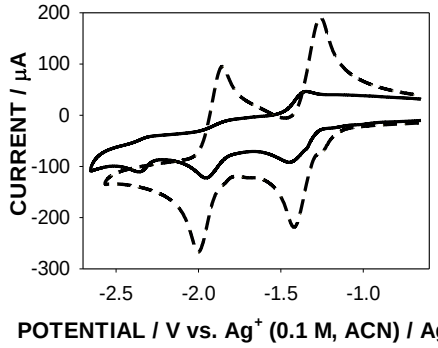

Figure 3. CVs measured for the residual solids isolated from the electrolyzed solutions. Electrolysis performed in the absence (——) or in the presence (— —) of an excess of CH_3I in the electrolytic media. Scan rate: 0.2 V/s. Electrolyte: 0.1M $NaClO_4$ in DMF.

The workup of the solutions resulting of the CPEs performed in the presence of CH_3I without or with added H_2O yields a solid which is identified (TLC and CG-MS) as NMI in quantitative molar yield, and 1 mol e^-/mol of electrolyzed ISH is consumed to generate in the medium the anion radical $ISH^{\bullet -}$. On the other hand, when the CPE is performed in the absence of the electrophilic reagent, and it is added to the electrolytic medium after the CPE is complete, NMIA is formed in addition to NMI, both products with *ca.* 50% molar yields (Table 1). Based on the identity and the molar yield of the reaction products, the current efficiency, and the CV behavior, possible reaction pathways (Scheme 2) are proposed for the electrolysis performed in EC1 and EC2 (Table 1). The formation of NMIA is explained in Scheme 2. The nucleophilic anion ISH^- reacts with the keto-carbonyl group of the ISH molecule to form a new dimeric anion (**1**, Scheme 2). During the workup of the electrolyzed solution carried out in an open atmosphere, **1** is oxidized in the presence of atmospheric oxygen giving rise to the radical **2** and the superoxide anion. Superoxide anion is coupled with **2** to form a molozonide species (**3**, Scheme 2),[52] which evolves to the ozonide. In the presence of CH_3I and the water from the environment, ozonide hydrolysis takes place to finally produce NMIA. The remaining *N*-anion is converted to NMI by the excess of CH_3I. Other authors have shown that in the absence of CH_3I, the preparative cathodic reduction of ISH leads to the formation of tryptanthrin (Figure 1).[48] In our work, we have not isolated any reaction intermediate, and from this point of view it might be possible that the proposed mechanism was not adequate. However, we consider that the possible mechanism published by Batanero and Barba[48] has been at present accepted by the scientific community. We have not detected tryptanthin in the experiment performed without MeI in the catholyte. No significant changes in the results of the quali/quantitative analyses of the isolated reaction products are observed when the electrolysis is carried out in the presence of water (Table 1). This result shows that NMIA is originated during the workup of the electrolyzed solution.

In our procedure, the methylation of ISH is explained through the generation of $ISH^{\bullet -}$ by the electrochemical way. This methodology employs the electron as a reagent, and does not require the use of temperature for the formation of the reactive species to methylation. The yield of NMI is not modified in the presence of an excess of water in the electrolyte medium and thus the use of anhydrous solvents is not necessary. However, to obtain NMI with the highest molar yield it is necessary to perform the CPE in the presence of the methylating agent. The electrolysis time 515 min (Table 1) was the time needed to electrolyze ISH in the presence of MeI and specially added H_2O to study its effect on the electrochemical behavior. In this condition, a portion of the circulated charge is consumed by the electrolysis of the H_2O and a decrease in the current efficiency is observed comparing with the experiment performed without added H_2O. In the absence of added H_2O to the electrolyte system, the electrolysis time was 115 min (Table 1), and the current efficiency for NMI was 100%. The molar yield for NMI was quantitative for both experiments. The apparent inconvenient of relative electrolysis long time (see Table 1) could be easily resolved by changing of the electrochemical experimental conditions as the area of the used electrode, the concentration of the electroactive substrate, the design of the electrolytic cell, and the agitation speed, which favors the mass transport from the bulk of the solution to the electrode/solution interface. These conditions can be adjustable so that the electrolysis reaction time can be shortened.

Scheme 2. Reaction mechanism proposed for the synthesis of NMI and NMIA.

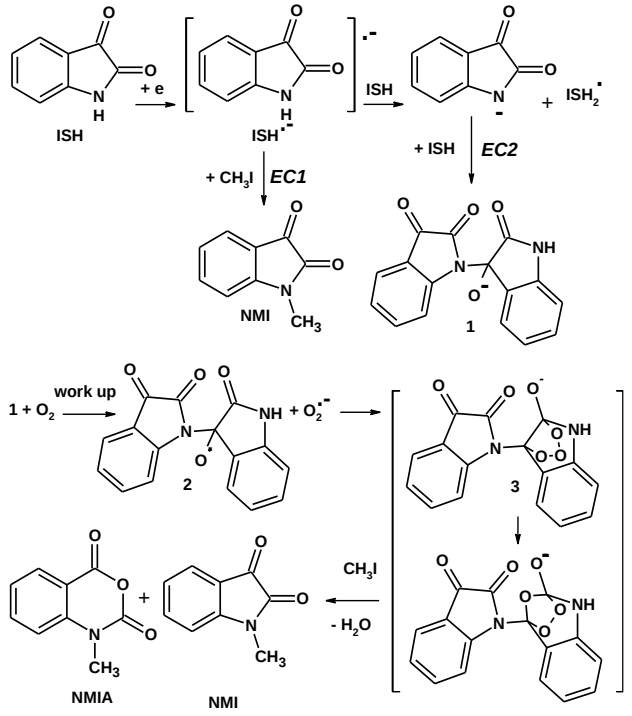

Physical properties and spectroscopic data measured for NMI synthesized in this work were compared with those of the authentic sample and with data previously published by other authors[28,32] and found to be identical. We carried out the search of NMI structure in Cambridge Structural Database (CCDC) and only found a single crystal X-ray analysis performed to confirm the structure of an unexpected reaction product that was identified as NMI.[53] While our manuscript was being sent to be considered for publication, Kumar et al.[54] published the crystal structure of NMI crystallized from methanol, without reporting the CCDC number. The results obtained by Kumar et al. and by us are similar, but they do not associate the intense color of NMI with its crystalline structure. Our detailed X-ray report (Table 2S) is presented in SI. A single crystal of NMI, obtained from CH_2Cl_2 solution by slow evaporation of the solvent, is shown in Figure 4a. The X-ray diffraction pattern shows that NMI crystallizes as a dimer and it does not include the solvent molecule.

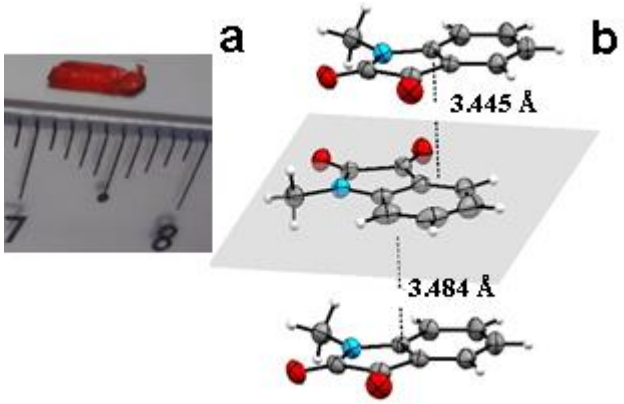

Figure 4. a) Single-crystal of NMI. b) View showing the dimeric arrangement of the two independent molecules in the asymmetric unit (upper pair of molecules) of solid state NMI. The bottom molecule is obtained from the upper one through a unit cell translation along the crystal a-axis. The displacement ellipsoids are drawn at the 30% probability level. The intra- and inter-dimer separations (in Å) correspond to distances from the centroids of the upper and bottom molecules to the plane through the middle one. Carbon, oxygen and nitrogen atoms are indicated by grey, red and blue colors, respectively.

Figure 4b shows a MERCURY[55] drawing of the solid state molecule. Intra-molecular bond distances an angles are in Table 3S. There are two chemically identical but crystallographically different molecules per asymmetric unit (space group P21/c, Z = 8). The intra-molecular geometry and metrics conform what is expected from established Organic Chemistry knowledge. Particularly, and because extended intra-molecular π-bonding delocalization, they are planar (rms deviation of non-H atoms from the least-squares plane less than 0.024 Å). The molecules are nearly parallel and rotated roughly 90º to each other and about 3.445 Å apart to conform a dimeric arrangement. Through unit cell translations along the short crystal a-axis, the dimers are piled-up about 3.484 Å apart in a canted fashion along this axis. The short inter-planar distances and significant molecular framework overlap favor considerable intermolecular π-π interaction which could explain the observed deep pink color exhibited by the solid (Figure 4a).

In conclusion, we have developed an electrochemically induced synthesis of NMI from ISH in DMF/$NaClO_4$ as supporting electrolyte system on carbon vitreous electrode, in the absence or in the presence of CH_3I and/or H_2O, using the CPE technique. Results show that there is an effect of the experimental conditions. NMI in quantitative molar yield and maximum current efficiency is obtained as the only reaction product in CPE performed in the presence of CH_3I in the electrolyte system. However, two products, NMI and NMIA are obtained in CPE performed in the absence of CH_3I, but adding it once the CPE was completed. On the other hand, there is not a water effect on the identity and molar yield of the products. The oxidized species NMIA is originated during the workup of the electrolyzed solution. Reaction pathways are proposed for the formation of these products. Our protocol provides an appealing approach to NMI synthesis, as it proceeds at room temperature, without the use of an external reducing agent or anhydrous organic solvents.

EXPERIMENTAL SECTION

General information. The reagents and solvents were of analytical grade. Isatin (Merck) was purified by recrystallization, [56] until constant melting point (m.p. 202-204 °C; Lit. [56] 201-203 °C). Commercial N-methyl isatin (Merck) was purified by recrystallization[57] (m.p. 131-132 °C; Lit.[32] 129-130 °C). Methyl iodide (Merck) and N-methylisatoic anhydride (high purity, ThermoFisher, Scientific) were employed as received without further purification. DMF puriss. p.a. (Merck) was dried with freshly activated 4Å molecular sieves and stored in the dry glove-box on a freshly activated molecular sieve. Its water content, measured by Karl-Fischer titration, was <50 ppm. Preparation of the solutions and electrochemical experiments were carried out inside a dry glove-box under a dry oxygen free nitrogen atmosphere.

ESR spectra were obtained at room temperature in a Bruker EMX-Plus spectrometer, using the 9.7 GHz frequency. The samples were held in 1mm diameter flame sealed glass capillaries. The simulated ESR spectra were computed with the Easy Spin program.[58,59] FT-IR spectra were recorded in KBr pellets on a Nicolet 380 FT-IR spectrophotometer,

equipped with a cryogenic MCT-A detector, cooled with liquid nitrogen and purged with dry air. The measurements were made at frequencies between 4000-400 cm^{-1}. GC-MS analyses were carried out in a Thermo Quest Trace model 2000, on a capillary column ZB-5HT Inferno (5% biphenyl, 95% polydimethylsiloxane), 30 m length, 0.32 mm internal diameter and 0.25 µm of stationary phase thickness, and helium was used as the carrier gas at 1mL/min. The mass detector was found with an electron ionization source (EI) and in acquisition mode SCAN at 70 eV. Silica-gel plates F_{254}Merck were used for TLC, and toluene/acetone (1:1 v/v) as the eluent solvent. Melting points were determined using the capillary tube method by a Melting Point Apparatus B-545 (Büchi, Flawil, Switzerland) and are uncorrected.

*Cyclic voltammetry (*CV*).* The CV experiments were performed in a conventional undivided gas-tight glass cell with dry nitrogen gas inlet and outlet. The working electrode was a 3 mm diameter vitreous carbon disk encapsulated in Teflon, the counter-electrode was a 2 cm^2 Pt foil, and an Ag^+ (0.1 M, ACN)/Ag reference electrode (to which all potentials reported are referred) was used. $NaClO_4$ was the supporting electrolyte. A LYP-M2 potentiostat, a 3-module LYP sweep generator and a WinPCChrom digital Data Acquisition Module were used.

X-ray diffraction data. The measurements were performed on an Oxford Xcalibur, Eos, Gemini CCD diffractometer with graphite-monochromated CuKα (λ = 1.54184 Å) radiation. X-ray diffraction intensities were collected (ω scans with ϑ and κ-offsets), integrated and scaled with CrysAlisPro[60] suite of programs. The unit cell parameters were obtained by least-squares refinement (based on the angular settings for all collected reflections with intensities larger than seven times the standard deviation of measurement errors) using CrysAlisPro. Data were corrected empirically for absorption employing the multi-scan method implemented in CrysAlisPro. The structure was solved by direct methods with the SHELXS program of the SHELX package[61] and the corresponding molecular models developed by alternated cycles of Fourier methods and full-matrix least-squares refinement with the program SHELXL of the same package. All H-atoms were determined from a Fourier difference map phased on the heavier atoms and refined at their found locations with isotropic displacement parameters. Crystal data, data collection procedure, and refinement results are summarized in Table 2S. CCDC number for the structure of NMI is 1829157.

General procedure for the electrosynthesis. Controlled potential electrolysis (CPE) of isatin (ISH) in dry DFM/$NaClO_4$ as solvent-supporting electrolyte system on a carbon vitreous electrode was performed in the absence and in the presence of an excess of water, in the presence of methyl iodide (CH_3I) and in the absence of the methylating agent in the electrolyte solution (see EC1 and EC2 in Table 1). An excess of CH_3I was immediately added to the electrolyte solution when the CPE performed in the absence of this agent was completed.

The general procedure adapted for each case was the following: ISH (128 mg; 0.87 mmol) in 0.1M $NaClO_4$/DMF (85 mL) as the electrolyte solution was added to the cathode compartment of the cell. For the CPE performed in the presence of the methylating agent, 80µL of CH_3I were added, and/or 77 µL of H_2O (4.28 mmol) for the assays performed in its presence. The applied potential was -1.35 V (*vs.* Ag^+ (0.1 M, ACN)/Ag°)). The progress of the CPE was performed by TLC and CV. In all cases, the circulated current intensity (I) was recorded as a function of the electrolysis time (t_{elect}). When $I_{final}<1\%I_{initial}$ the electrolysis was ended. The solution electrolyzed in the absence of CH_3I showed an intense violet color at the end of the electrolysis. A change in the coloration of the solution to yellow-brown was observed after CH_3I addition (15 mM). In all experiments the resulting cathodic solution was worked up, first removing the DMF solvent (2 mm Hg, 50 ºC), DCM was added to the residual solid and the suspension was stored at 4 °C, for 24 h. The insoluble supporting electrolyte was separated by filtration and washed with DCM that was added to the filtered solution. DCM of the combined organic extracts was removed and the residual solid was dried. Its purity was checked by TLC and by gas chromatography coupled to a mass spectrometer (GC/MS). The reaction products were identified by GC/MS, TLC, mixed melting point and FT-IR by comparison with authentic samples. The electrochemical characterization was performed by CV inside a glove-box, under a dry oxygen-free N_2 atmosphere.

The electrolysis cell, the electrolyzed solutions and all the laboratory material used were covered with aluminium foil to prevent possible photochemistry of the reagents and/or products.[62-64]

*1-methylindoline-2,3-dione (*NMI*).* Yellow crystalline solid, (100% yield, 140.2 mg); m.p. 130–132 ºC. *m/z* (EI) 161.0; ν_{max} (cm^{-1}) 3054, 2923, 1742, 1723, 1599, 1467, 1091. *See also*: Figure 8S, Part I; Table 1S, Part II.

ASSOCIATED CONTENT

Supporting Information

The Supporting Information (SI) is available free of charge on the ACS Publications website.

X-ray crystallography data for compound NMI (CIF)

Crystal data of NMI, CV and GC-MS of the reaction products (PDF)

AUTHOR INFORMATION

Corresponding Author

*Email: mirifi@live.com.ar ; mirifi@inifta.unlp.edu.ar

ORCID

Jaime F. Martínez Suárez: 0000-0003-2381-3509
Ana María Gennaro: 0000-0003-0309-8819
María V. Mirífico: 0000-0001-6093-2211

Notes

The authors declare no competing financial interest.

Author Contributions

All authors have given approval to the final version of the manuscript.

ACKNOWLEDGMENT

This work was financially supported by Consejo Nacional de Investigaciones Científicas y Técnicas (CONICET, CCT LP) and Universidad Nacional de La Plata (UNLP), Facultad de Ciencias Exactas, Departamento de Química and Facultad de Ingeniería, Departamento de Ingeniería Química. M. V. M, J. A. C., E. O. P. and G. A. E. are researchers of CONICET and UNLP; A. M. G. is researcher of CONICET and UNL; J. F. M. S. is a doctoral fellow of CONICET.

REFERENCES

(1) Lee, D.; Long, S. a; Murray, J. H.; Adams, J. L.; E, M.; Nadeau, D. P.; Kikly, K.; Winkler, J. D.; Sung, C.; Ryan, M. D.; et al. Potent and Selective Nonpeptide Inhibitors of Caspases 3 and 7. *J. Med. Chem.* **2001**, *44*, 2015–2026. https://doi.org/10.1021/jm0100537.

(2) Chapman, J. G.; Magee, W. P.; Stukenbrok, H. A.; Beckius, G. E.; Milici, A. J.; Tracey, W. R. A Novel Nonpeptidic Caspase-3/7 Inhibitor, (S)-(+)-5-[1-(2-Methoxymethylpyrrolidinyl)Sulfonyl]Isatin Reduces Myocardial Ischemic Injury. *Eur. J. Pharmacol.* **2002**, *456*, 59–68. https://doi.org/10.1016/S0014-2999(02)02484-6.

(3) Cheke, R. S.; Firke, S. D.; Patil, R. R.; Bari., S. B. ISATIN: New Hope Against Convulsion. *Cent. Nerv. Syst. Agents Med. Chem.* **2018**, *18* (2), 76–101. https://doi.org/10.2174/1871524917666171113124112.

(4) Sriram, D.; Bal, T. R.; Yogeeswari, P. Design, Synthesis and Biological Evaluation of Novel Non-Nucleoside HIV-1 Reverse Transcriptase Inhibitors with Broad-Spectrum Chemotherapeutic Properties. *Bioorganic Med. Chem.* **2004**, *12*, 5865–5873. https://doi.org/10.1016/j.bmc.2004.08.028.

(5) Pirrung, M. C.; Pansare, S. V; Sarma, K. Das; Keith, K. a; Kern, E. R. Combinatorial Optimization of Isatin-ß-Thiosemicarbazones as Anti-Poxvirus Agents. *J. Med. Chem.* **2005**, *48*, 3045–3050. https://doi.org/10.1021/jm049147h.

(6) Chohan, Z. H.; Pervez, H.; Rauf, A.; Khan, K. M.; Supuran, C. T. Isatin-Derived Antibacterial and Antifungal Compounds and Their Transition Metal Complexes. *J. Enzyme Inhib. Med. Chem.* **2004**, *19* (5), 417–423. https://doi.org/10.1080/14756360410001710383.

(7) Walker, B.; Kim, C.; Nguyen, T. Q. Small Molecule Solution-Processed Bulk Heterojunction Solar Cells. *Chem. Mater.* **2011**, *23*, 470–482. https://doi.org/10.1021/cm102189g.

(8) Mishra, A.; Bäuerle, P. Small Molecule Organic Semiconductors on the Move: Promises for Future Solar Energy Technology. *Angew. Chemie - Int. Ed.* **2012**, *51* (9), 2020–2067. https://doi.org/10.1002/anie.201102326.

(9) Zhang, G.; Fu, Y.; Xie, Z.; Zhang, Q. Synthesis and Photovoltaic Properties of New Low Bandgap Isoindigo-Based Conjugated Polymers. *Macromolecules* **2011**, *44*, 1414–1420. https://doi.org/10.1021/ma102357b.

(10) Xu, X.; Li, L.; Liu, B.; Zou, Y. Organic Semiconductor Memory Devices Based on a Low-Band Gap Polyfluorene Derivative with Isoindigo as Electron-Trapping Moieties. *Appl. Phys. Lett.* **2011**, *98* (063303), 1–3. https://doi.org/10.1063/1.3554756.

(11) Lei, T.; Cao, Y.; Fan, Y.; Liu, C.; Yuan, S.; Pei, J. High-Performance Air-Stable Organic Field-Effect Transistors: Isoindigo-Based Conjugated Polymers. *J. Am. Chem. Soc.* **2011**, *133*, 6099–6101. https://doi.org/10.1021/ja111066r.

(12) Ashraf, R. S.; Kronemeijer, A. J.; James, D. I.; Sirringhaus, H.; McCulloch, I. A New Thiophene Substituted Isoindigo Based Copolymer for High Performance Ambipolar Transistors. *Chem. Commun.* **2012**, *48*, 3939–3941. https://doi.org/10.1039/c2cc30169e.

(13) Porada, J. H.; Blunk, D. Synthesis and Supramolecular Organization of 5- (4-Alkylphenyl) Isatin. *Cryst. Growth Des.* **2011**, *11*, 3648–3652. https://doi.org/10.1021/cg200700r.

(14) Yang, Y.; Shi, Z. Regioselective Direct Arylation of Indoles on the Benzenoid Moiety. *Chem. Commun.* **2018**, *54*, 1676–1685. https://doi.org/10.1039/c7cc08752g.

(15) Nogrady, T.; Donald, F. *Chimie Thérapeutique*, Third edit.; 2005.

(16) Kaushik, N. K.; Kaushik, N.; Attri, P.; Kumar, N.; Kim, C. H.; Verma, A. K.; Choi, E. H. Biomedical Importance of Indoles. *Molecules* **2013**, *18*, 6620–6662. https://doi.org/10.3390/molecules18066620.

(17) Singh, T. P.; Singh, O. M. Recent Progress in Biological Activities of Indole and Indole Alkaloids. *Mini-Reviews Med. Chem.* **2018**, *18*, 9–25. https://doi.org/10.2174/1389557517666170807123201.

(18) Vine, K. L.; Locke, J. M.; Ranson, M.; Benkendorff, K.; Pyne, S. G.; Bremner, J. B. In Vitro Cytotoxicity Evaluation of Some Substituted Isatin Derivatives. *Bioorganic Med. Chem.* **2007**, *15*, 931–938. https://doi.org/10.1016/j.bmc.2006.10.035.

(19) Giorno, T. B. S.; Silva, B. V. Da; Pinto, A. D. C.; Fernandes, P. D. Antinociceptive Effect and Mechanism of Action of Isatin, N-Methyl Isatin and Oxopropyl Isatin in Mice. *Life Sci.* **2016**, *151*, 189–198. https://doi.org/10.1016/j.lfs.2016.02.052.

(20) Chen, G.; Wang, Y.; Hao, X.; Mu, S.; Sun, Q. Simple Isatin Derivatives as Free Radical Scavengers: Synthesis, Biological Evaluation and Structure-Activity Relationship. *Chem. Cent. J.* **2011**, *5* (37), 1–5. https://doi.org/10.1186/1752-153X-5-37.

(21) Kang, I. J.; Wang, L. W.; Hsu, T. A.; Yueh, A.; Lee, C. C.; Lee, Y. C.; Lee, C. Y.; Chao, Y. S.; Shih, S. R.; Chern, J. H. Isatin-β-Thiosemicarbazones as Potent Herpes Simplex Virus Inhibitors. *Bioorganic Med. Chem. Lett.* **2011**, *21* (7), 1948–1952. https://doi.org/10.1016/j.bmcl.2011.02.037.

(22) Mishra, P.; Kumar, A.; Mamidi, P.; Kumar, S.; Basantray, I.; Saswat, T.; Das, I.; Nayak, T. K.; Chattopadhyay, S.; Subudhi, B. B.; et al. Inhibition of Chikungunya Virus Replication by 1-[(2-Methylbenzimidazol-1-Yl) Methyl]-2-Oxo-Indolin-3-Ylidene] Amino] Thiourea(MBZM-N-IBT). *Sci. Rep.* **2016**, *6* (July 2015), 1–13. https://doi.org/10.1038/srep20122.

(23) Kiran, G.; Maneshwar, T.; Rajeshwar, Y.; Sarangapani, M. Microwave-Assisted Synthesis, Characterization, Antimicrobial and Antioxidant Activity of Some New Isatin Derivatives. *J. Chem.* **2013**, *2013* (Article ID 192039), 1–7. https://doi.org/10.1155/2013/192039.

(24) Lee, S.; Lim, Y.; Jeon, Y.; Hossain, M. A.; Jang, H.; Cho, Y.; Kim, W. G. Synthesis and Properties of Sulfonated Poly(N-Methylisatin-Biphenylene) Proton Exchange Membrane by Superacid-Catalyzed Polymerization. *Int. J. Hydrogen Energy* **2015**, *40* (15), 5390–5395. https://doi.org/10.1016/j.ijhydene.2015.01.038.

(25) Carmen, M.; Herńandez, G.; Zolotukhin, G.; Luis, M.; Rehmann, N.; Meerholz, K.; King, S.; Monkman, A. P.; Fröhlich, N.; Kudla, C. J.; et al. A High Molecular Weight Aromatic PhOLED Matrix Polymer Obtained by Metal-Free, Superacid-Catalyzed Polyhydroxyalkylation. *Macromolecules* **2009**, *42* (23), 9225–9230. https://doi.org/10.1021/ma902061t.

(26) Bogdanov, A. V; Musin, L. I.; Mironov, V. F.; Arbuzov, A. E. Advances in the Synthesis and Application of Isoindigo Derivatives. *ARKIVOC* **2015**, *vi*, 362–392. https://doi.org/10.3998/ark.5550190.p009.090.

(27) Sword, R.; O'Sullivan, S.; Murphy, J. A. A Novel Organic Electron Donor Derived from N-Methylisatin. *Aust. J. Chem.* **2013**, *66* (3), 314–322. https://doi.org/10.1071/CH12480.

(28) Mahajan, P. G.; Bhopate, D. P.; Kolekar, G. B.; Patil, S. R. N-Methyl Isatin Nanoparticles as a Novel Probe for Selective Detection of Cd2+ Ion in Aqueous Medium Based on Chelation Enhanced Fluorescence and Application to Environmental Sample. *Sensors Actuators B Chem.* **2015**, *220*, 864–872. https://doi.org/http://dx.doi.org/10.1016/j.snb.2015.05.119.

(29) Da Silva, J. F. M.; Garden, S. J.; Pinto, A. C. The Chemistry of Isatins: A Review from 1975 to 1999. *J. Braz. Chem. Soc.* **2001**, *12* (3), 273–324. https://doi.org/10.1590/S0103-50532001000300002.

(30) Diaz, P.; Xu, J.; Astruc-Diaz, F.; Pan, H.-M.; Brown, D. L.; Naguib, M. Design and Synthesis of a Novel Series of *N* -Alkyl Isatin Acylhydrazone Derivatives That Act as Selective Cannabinoid Receptor 2 Agonists for the Treatment of Neuropathic Pain. *J. Med. Chem.* **2008**, *51* (16), 4932–4947. https://doi.org/10.1021/jm8002203.

(31) Farooq, M.; Almarhoon, Z. M.; Taha, N. A.; Baabbad, A. A. R.; Al-Wadaan, M. A.; El-Faham, A. Synthesis of Novel Class of N-Alkyl-Isatin-3-Iminobenzoic Acid Derivatives and Their Biological Activity in Zebrafish Embryos and Human Cancer Cell Lines. *Biol. Pharm. Bull.* **2018**, *41* (3), 350–359. https://doi.org/10.1248/bpb.b17-00674.

(32) Shmidt, M. S.; Reverdito, A. M.; Kremenchuzky, L.; Perillo, I. A. Simple and Efficient Microwave Assisted N-Alkylation of Isatin. *Molecules* **2008**, *13*, 831–840. https://doi.org/10.3390/molecules13040831.

(33) Al-Ayed, A. S.; Ali, M. S.; Al-Lohedan, H. a.; Al-Sulaim, A. M.; Issa, Z. a.; Kabir-ud-Din. Micellar Effects on the Alkaline Hydrolysis of Isatin and Its Derivatives. *J. Colloid Interface Sci.* **2011**, *357* (2), 393–399. https://doi.org/10.1016/j.jcis.2011.02.004.

(34) Radman, R. F.; Ismail, A. M.; Al-Jallal, N. a. Kinetics of the

Alkaline Hydrolysis of Isatin and N-Methylisatin in Water and Water-N,N-Dimethylacetamide Mixtures. *J. Saudi Chem. Soc.* **2010**, *14* (2), 223–229. https://doi.org/10.1016/j.jscs.2010.02.021.

(35) Torisawa, Y.; Nishi, T.; Minamikawa, J.-I. An Efficient Conversion of 5-Nitroisatin Into 5-Nitroindole Derivative. *Bioorg. Med. Chem. Lett.* **2001**, *11*, 829-832. doi: 10.1016/S0960-894X(01)00071-3

(36) Batanero, B.; Recio, J.; Barba, F. One-Pot Anodic Lactonization of Fenchone and Menthone and Electrosynthesis of a New Magnolione Analogue. *Electrochem. commun.* **2016**, *66*, 29–33. https://doi.org/10.1016/j.elecom.2016.02.018.

(37) Wallace, L. Electrochemical Methods for Synthesis of Energetic Materials and Remediation of Waste Water. In *Green Energetic Materials*; Brinck, T., Ed.; John Wiley & Sons Ltd, **2014**. https://doi.org/10.1002/9781118676448.ch10.

(38) Cardoso, D. S. P.; Šljukić, B.; Santos, D. M. F.; Sequeira, C. A. C. Organic Electrosynthesis: From Laboratorial Practice to Industrial Applications. *Org. Process Res. Dev.* **2017**, *21* (9), 1213–1226. https://doi.org/10.1021/acs.oprd.7b00004.

(39) Francke, R.; Little, R. D. Redox Catalysis in Organic Electrosynthesis: Basic Principles and Recent Developments. *Chem. Soc. Rev.* **2014**, *43*, 2492–2521. https://doi.org/10.1039/C3CS60464K.

(40) Tang, S.; Liu, Y.; Lei, A. Electrochemical Oxidative Cross-Coupling with Hydrogen Evolution: A Green and Sustainable Way for Bond Formation. *Chem* **2018**, *4* (1), 27–45. https://doi.org/10.1016/j.chempr.2017.10.001.

(41) Nicholson, R. S.; Shain, I. Theory of Stationary Electrode Polarography: Single Scan and Cyclic Methods Applied to Reversible, Irreversible, and Kinetic Systems. *Anal. Chem.* **1964**, *36* (4), 706–723. https://doi.org/10.1021/ac60210a007.

(42) Farnia, G.; Capobianco, G.; Romanin, A. Polarographic Behaviour of Isatin and Some of Its Derivatives in DMF. *Electroanal. Chem. Interfacial Electrochem.* **1973**, *45*, 397–404. https://doi.org/10.1016/S0022-0728(73)80049-X.

(43) Gupta, A. K,; Sindal R. S. A comparative study of electrochemical reduction of isatin and its synthesized Schift bases ay HDME. *J. Chem. Sci.* **2009**, *121* (3), 347-351.

(44) Given, P. H.; Peover, M. E.; Schoen, J. Polarography of Some Aromatic Carbonyl Compounds in Dimethylformamide. *J. Chem. Soc.* **1958**, 2674–2679. https://doi.org/10.1039/JR9580002674.

(45) Guin, P. S.; Das, S.; Mandal, P. C. Electrochemical Reduction of Quinones in Different Media: A Review. *Int. J. Electrochem.* **2011**, *2011*, 1–22. https://doi.org/10.4061/2011/816202.

(46) Caram, J. A.; Banera, M. J.; Martínez Suárez J. F.; Mirífico M. V. Electrochemical behaviour of anthraquinone dyes in non-aqueous solvent solution. *Electrochim. Acta*, **2017**, *249*, 431-445. http://dx.doi.org/10.1016/j.electacta.2017.07.139.

(47) Caram J. A.; Mirífico M. V.; Vasini E. J. Electrochemistry of 3,4-diphenyl-1,2,5-thiadiazole-1,1-dioxide (I) and its derivatives in ethanol-acetonitrile solutions and interactions of the dianion of I with metal cations. *Electrochim. Acta*, **1994**, *39* (7), 939-945. https://doi.org/10.1016/0013-4686(94)85109-3.

(48) Batanero, B.; Barba, F. Electrosynthesis of Tryptanthrin. *Tetrahedron Lett.* **2006**, *47* (47), 8201–8203. https://doi.org/10.1016/j.tetlet.2006.09.130.

(49) Todres Z. V., Ion-Radical Organic Chemistry Principles and Applications, CRC Press, Taylor & Francis Group. Boca Raton London New York, Second Edition, **2009**.

(50) Caram J. A.; Jiménez Macías J. P; Rodríguez Arroyo N.; Martínes Suárez J. F.; Gennaro A. M.; Piro O. E.; Mirífico M. V. Stability of the Monoelectronic Reduction Product from 1,2,5-Thiadiazole S,S-Dioxides. Electrochemical, Chemical, and Photoinduced Doping, *ChemistrySelect*, **2018**, *3*, 8729 – 8739. https://doi.org/10.1002/slct.201801237.

(51) Farinia G.; Capobianco G.; Romanin A. Polarographic behaviour of isatin and some of its derivatives in DMF. *Electroanal. Chem. Interf Electrochem.*, **1973**, *45*, 397-404. https://doi.org/10.1016/S0022-0728(73)80049-X.

(52) Swern, D. *Organic Peroxides*; Wiley Interscience. Wiley and Sons, **1971**; Vol. II.

(53) Gao, X. A.; Yan, R. L.; Wang, X. X.; Yan, H.; Li, J.; Guo, H.; Huang, G. S. Pd(II)-Catalyzed Synthesis of Benzisoxazolones from Benzohydroxamic Acids via C-H Activation. *J. Org. Chem.* **2012**, *77*, 7700–7705. https://doi.org/10.1021/jo301180k.

(54) Kumar Swamy S. R.; Hema M. K.; Mahesha; Pampa K. J.; Lokanath N. K. Crystal Structure, Hirshfeld Surface Analysis, Energy Frameworks and DFT Studies of 1-methylindoline-2, 3-Dione. *Journal of Applicable Chemistry*, **2018**, *7* (6), 1747-1754.

(55) Macrae, C. F.; Edgington, P. R.; McCabe, P.; Pidcock, E.; Shields, G. P.; Taylor, R.; Towler, M.; Van De Streek, J. Mercury: Visualization and Analysis of Crystal Structures. *J. Appl. Crystallogr.* **2006**, *39* (3), 453–457. https://doi.org/10.1107/S002188980600731X.

(56) Armarego, W. L. F. *Purification of Laboratory Chemicals*, Eighth Edi.; Elsevier Inc., 2017. https://doi.org/10.1016/S0022-328X(00)82974-5.

(57) Thanh, N. D.; Giang, N. T. K. Reaction of N-Alkylisatins with 4-(2,3,4,6-Tetra-O-Acetyl--D-Glucopyranosyl)Thiosemicarbazide. *J. Chem.* **2013**, *2013* (Article ID 237058), 1–5. https://doi.org/10.1155/2013/237058.

(58) Stoll, S.; Schweiger, A. EasySpin, a Comprehensive Software Package for Spectral Simulation and Analysis in EPR. *J. Magn. Reson.* **2006**, *178*, 42–55. https://doi.org/10.1016/j.jmr.2005.08.013.

(59) Stoll, S.; Schweiger, A. Easyspin: Simulating Cw ESR Spectra. In *Biological Magnetic Resonance*; Springer Science+Business Media, **2007**; pp 299–321.

(60) Oxford Diffraction Ltd. CrysAlisPro. 15-09-2009 CrysAlis171.NET **2009**.

(61) Sheldrick, G. M. A Short History of SHELX. *Acta Crystallogr.* **2008**, *A64*, 112–122. https://doi.org/10.1107/S0108767307043930.

(62) Haucke, G.; Seidel, B.; Graness, A. The Photochemistry of Isatin. *J. Photochem.* **1987**, *37*, 139–146. https://doi.org/10.1016/0047-2670(87)85035-9.

(63) Sharma, I.; Saxena, A.; Ojha, C. K.; Pardasani, P.; Pardasani, R. T.; Mukherjee, T. A Comprehensive Approach to the Photochemical Synthesis of Bioactive Compounds by the Reaction of Oxazolidine, Thiazolidine and Pyrazolidine Derivatives with Indol-2,3-Diones. *Proc. Indian Acad. Sci. Chem. Sci.* **2002**, *114* (6), 523–531. https://doi.org/10.1007/BF02708846.

(64) Silva, M. T.; Netto-Ferreira, J. C. Laser Flash Photolysis Study of the Photochemistry of Isatin and N-Methylisatin. *J. Photochem. Photobiol. A Chem.* **2004**, *162*, 225–229. https://doi.org/10.1016/S1010-6030(03)00383-6.